e-ISSN: 2757-9077

Open Access

ENGINEERING PERSPECTIVE

CONTENTS

ENGINEERING PERSPECTIVE Volume: 3 Issue: 2 30 June 2023

ENGINEERING PERSPECTIVE

An International Journal

Volume: 3 Issue: 2 30 June 2023

https://sciperspective.com

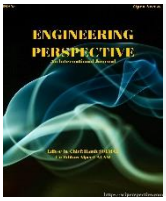

ISSN: 2757-9077

ENGINEERING PERSPECTIVE

https://sciperspective.com/ Research Paper

Modeling the Vehicle Movement and Braking Effect of the Hydrostatic Regenerative Braking System

Mustafa Karaman[1,3*], Salih Korucu[2]

[1]*Manufacturing Engineering, Graduate School of Natural and Applied Sciences, Gazi University, Ankara, 06500, Turkey*
[2] *Manufacturing Engineering, Faculty of Technology, Gazi University, Ankara, 06500, Turkey*
[3] *Hidroan Ankara Hidrolik Mak. San. Tic. Ltd. Şti, Ankara, 06374, Turkey*

ABSTRACT

In this study, the main elements of a hydrostatic regenerative braking system have been modeled. The model which has been created, the elements in the system and the relationship of the system with the vehicle has been studied. In order to measure the performance of the regenerative system, driving cycles for accelerating and stopping the vehicle using only the hydraulic system have been simulated. Simulation studies have indicated that by using this system, a vehicle such as a heavy truck can be accelerated up to 4m/s velocity and moved more than 100m. The energy needed for this motion can again be stored by the regenerative braking system. Results indicate that accumulator can be fully charged in seconds with initial speed of 15 m/s. This model can be used in determining hydraulic elements that can be used in experimental studies. The calculation of losses is also planned to be incorporated to the model in the future.

Keywords: Hydrostatic Regenerative Braking System, Hybrid Vehicle, Hydraulic Hybrids, hydraulic system modeling, accumulator modeling

History
Received: 07.02.2023
Accepted: 18.05.2023

How to cite this paper: Karaman, M., Korucu., S., (2023), Modeling the Vehicle Movement and Braking Effect of the Hydrostatic Regenerative Braking System. Engineering Perspective, 3(2), 18-27. http://dx.doi.org/10.29228/eng.pers.69826

Author Contacts
**Corresponding Author*
e-mail addresses : mkaraman@hidroan.com.tr, skorucu@gazi.edu.tr

1. Introduction

Environmental and climate worries have given rise to the automotive industry to look for new technologies to reduce fuel consumption. Industry and institutions have developed numerous energy recovery systems to satisfy this need. Energy recovery systems serve similar purposes towards the regenerative braking systems [1]. In vehicles with internal combustion engines, these systems are classified into three distinct categories: exhaust-based, vertical-release and vehicle-based energy retrieval systems.

Hydraulic-pneumatic energy retrieval systems (hydrostatic regenerative braking systems) are an example of systems that enables energy-retrieval by the vehicle. In the parallel hydrostatic regenerative braking system in Figure 1, energy is stored by compressing the nitrogen gas in the hydraulic accumulator. The pressure generated by the compressed gas whenever needed, the hydraulic fluid is used to transmit to the hydraulic pump/motor drive that is connected to the vehicle's power transmission system. It is possible to move the vehicle with this hydraulic motor. During braking, the hydraulic pump/motor element is used in pump mode to transmit hydraulic fluid to the accumulator. The oil transmitted to the accumulator compresses the nitrogen gas. In this way, the kinetic energy of the vehicle is stored as gas pressure. Energy storage by compression of nitrogen gas is called hydraulic regeneration, the braking process at the same time is called hydrostatic braking [2].

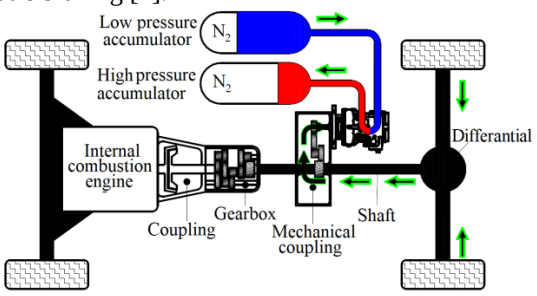

Figure 1. Parallel hydrostatic regenerative braking system

Fuel cells and batteries used for energy storage have a low power density due to their high internal resistance. In contrast, hydraulic accumulators have a lower energy density compared to the technologies used for electrical storage, as well as high power density. The Ragone diagram in Figure 2 demonstrates a comparison of different energy storage technologies in terms of energy and power density. In terms of retrieval of braking energy, especially in commercial vehicles, hydraulic accumulators put forward a significant advantage in power density compared to electric batteries [3].

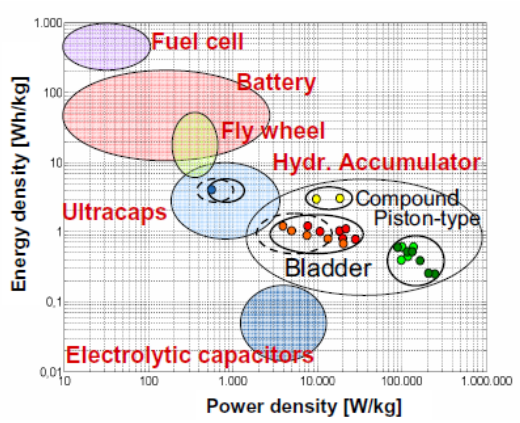

Figure 2. Ragone diagram showing comparison of different energy storage technologies [3].

Hydraulic systems having power density advantage by using energy storage is also available where energy is converted into motion. For example, the power density of hydromotors is greater than that of electric motors. Comparison of the different characteristics of hydraulic and electronic systems are shown in Table 1 and 2.

Table 1. Comparison of electric motor and hydraulic engine performance [4].

Performance	Electric Motor	Hydro motors
Power Density	0.5 kW/kg	>4 kW/kg
%20 Load Efficiency	%90	%93
Cost	1 / kW	0.3 / kW

Table 2. Comparison of hydraulic accumulator and electric battery [4].

Energy Storage Performance	Hydraulic Accumulator	Electric Battery
Power Density	5 kW/kg	0.5 kW/kg
Energy Density	4-111 kJ/kg	150 kJ/kg
Reverse Efficiency	%94	%81

As hydraulic energy retrieval systems can be implemented to vehicles such as a garbage truck having a mechanical transmission, they can also be easily integrated into heavy construction machines such as diggers with a hydraulic drivetrain This means that hydraulic systems also contribute various facilities in terms of application in addition to the advantages shown in the tables. The simplified diagrams describing the working principle of the supplementary and integrated systems mentioned above are shown in Figure 3.

These advantages of hydraulic energy retrieval systems have put forward numerous research on the topic. For example, in 2011, Ho and Ahn demonstrated that the retrieval efficiency could reach up to 59% in their study taking into consideration the design and control of a closed-circuit hydraulic energy retrieval system. In their 2014 study, Shen and his colleagues demonstrated that the fuel consumption of a hydraulic hybrid excavator can be significantly reduced with correct control variables [6]. In a study conducted by Liu and his colleagues in 2019 by using railed vehicles with electro-hydrostatic power transmission systems, they demonstrated that energy retrieval performance can go up to 40% in low tilt conditions, on other hand go up to 20% in high tilt conditions compared to vehicles with only electric drive systems [7].

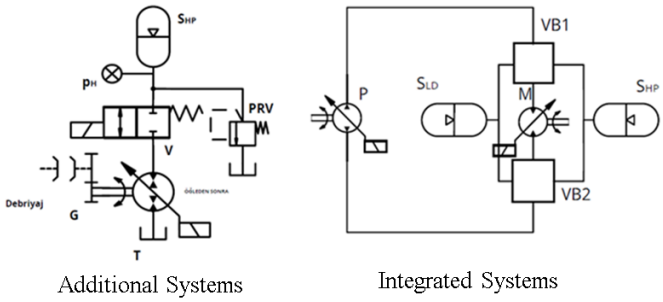

Figure 3. Additional and integrated systems scheme [3].

A mathematical model of a hydraulic energy retrieval system, which is planned to be installed as an additional system on a vehicle (e.g. a garbage truck) with a load weight of 18,000 kg and which frequently stops and takes off is developed in this study. The presented model examines the vehicle's stopping and taking off through the hydraulic system under various conditions such as charge the accumulator and different initial speeds. Vehicle parameters such as hydraulic pump/motor displacement, transmission rate and efficiency have been determined in the model by using similar vehicles.

2. Mathematical model

For the creation of the mathematical model, the resistance forces affecting the vehicle and the force applied by the hydraulic system have been considered. The acceleration of the vehicle can be calculated by the equation number (1).

$$ma = F_H - F_D \quad (1)$$

In equation (1) m represents the mass of the vehicle, a represents acceleration, F_H is the force applied by the hydraulic system, on the other hand F_D is the sum of the resistive forces. After the acceleration of the vehicle is determined by the force balance, the speed and change of the position can also be found by taking the time-dependent integral. The acceleration of the vehicle by using mass weight can be seen on Figure 4 MATLAB–Simulink.

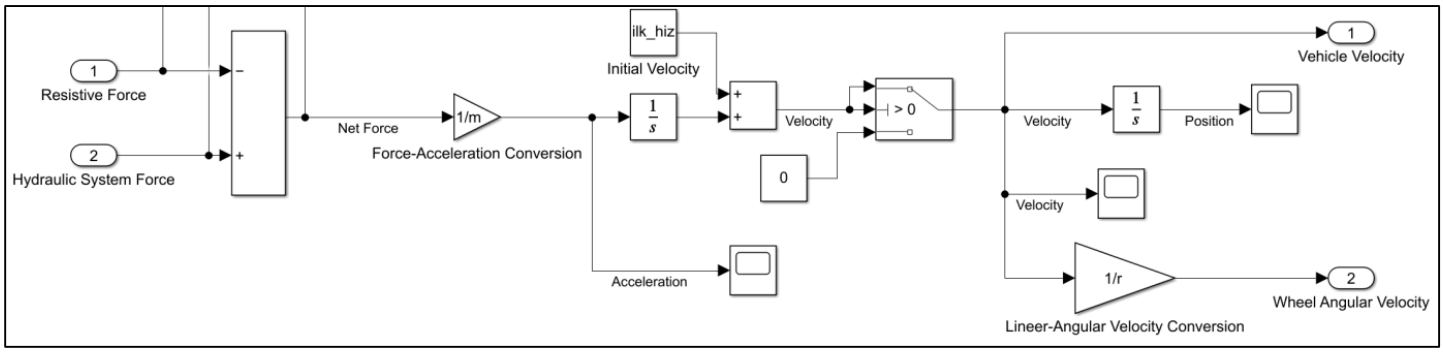

Figure 4. Vehicle acceleration, speed and location MATLAB-Simulink model

2.1. Resistive forces acting on the vehicle

During the movement the vehicle is exposed to some resistive forces. Resistive forces are forces formed by various factors in the opposite direction towards the movement of the vehicle. The resistance forces under the influence of the vehicle are rolling, aerodynamic and weight resistance [8]. These forces are shown in Figure 5.

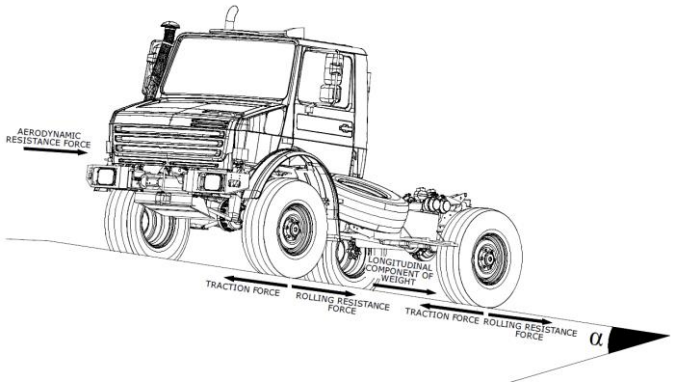

Figure 5. Resistance forces affecting the vehicle.

The sum of the forces affecting the vehicle has been expressed as F_D equation (1) and is calculated as shown in the equation (2).

$$F_D = F_r + F_a + F_y \quad (2)$$

In equation (2) F_r represents the rolling resistance corresponding to the rotation movement of the wheel. Rolling resistance, due to the elastic structure of the wheel is the resistance force formed in front of the contact center, against the rotation movement of the Wheel. The rolling resistance coefficient C_r is directly influenced by parameters such as vehicle mass, tire type, tire air pressure and road conditions and can be calculated using the equation (3).

$$F_r = m \cdot g \cdot C_r \cdot \cos\alpha \quad (3)$$

In equation (3) the g represents gravitational acceleration , a presents the angle of the inclination of the ground in which the vehicle is moving.

The air flow that the vehicle encounters during movement creates a force in the opposite direction of the vehicle. This force in the opposite direction of the vehicle's movement is called aerodynamic resistance [9]. F_a indicates the aerodynamic resistance force on the vehicle and is calculated as expressed in equation 4.

$$F_a = C_d \cdot \frac{\rho v^2}{2} \cdot A \quad (4)$$

In equation (4), C_d refers to the aerodynamic friction coefficient, ρ air density, $\mathcal{V}$ represents the speed of the vehicle and A represents the cross-sectional area of the vehicle.

Weight resistance is the force that occurs due to the longitudinal component of the weight of vehicle on the inclined road. This resistance is directly related to the mass of the vehicle and the tilt of the slope [10]. F_y symbolizes the resistive force and is calculated as shown in equation 5.

$$F_y = m \cdot g \cdot \sin\alpha \quad (5)$$

The MATLAB-Simulink model used for calculating the resistive forces acting on the vehicle is shown in Figure 6.

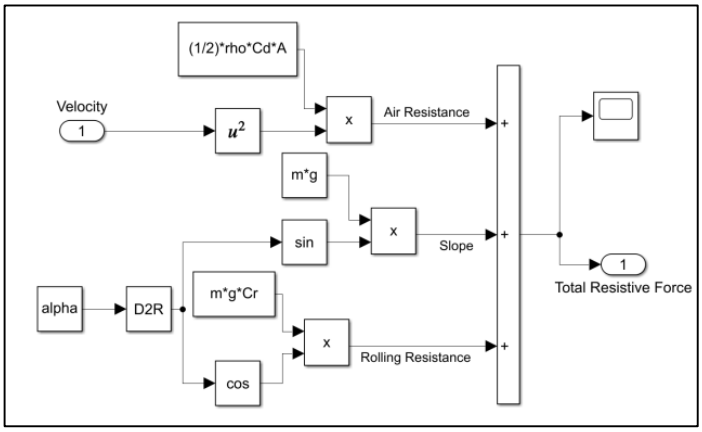

Figure 6. The Matlab-Simulink Resistive Forces Model.

2.2. Hydraulic system and vehicle relationship

Variables such as the force and the flow rate applied by the hydraulic system to the vehicle are directly related to the shaft speed of the hydraulic pump/motor element. A system which connects the wheel axis to the pump/motor axis can be considered directly establish the relationship between shaft speed of the pump / motor element and vehicle speed. A simplified representation

describing the connection between the pump/motor element and the wheel axis is shown in Figure 7.

The hydraulic pump/motor element is intermittently connected to the vehicle's drive shaft using transmission. The transfer rate of this intermediate transmission will be expressed as I_{kp}, efficiency by η_{kp}. Similarly, the wheel axle is connected to the vehicle drive shaft through differential. The transfer rate of the differential will be displayed as I_{df} and the efficiency will be η_{df}. The ratio between the torque generated by the pump/motor element and the one-axle torque is given in the equation (6).

$$T_{aks} = T_{hm} \cdot I_{kp} \cdot \eta_{kp} \cdot I_{df} \cdot \eta_{df} \quad (6)$$

In equation (6), the torque generated by the T_{hm} pump/motor element refers to the torque produced by T_{aks} wheel axle.

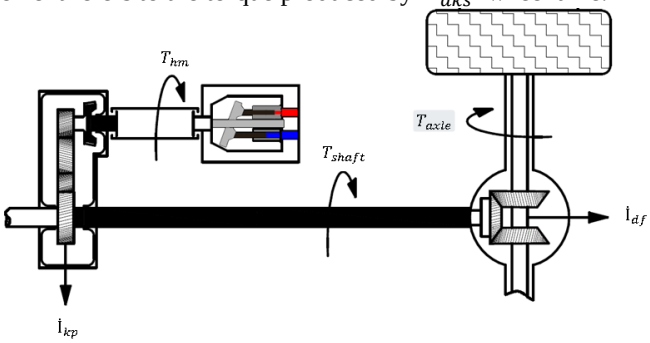

Figure 7. Wheel axle and pump/motor element shaft connection

Similarly, the relationship between the rotational velocity of the pump/motor component and the wheel axle rotational velocity is shown in the equation (7).

$$\omega_{aks} = \frac{\omega_{hm}}{I_{kp} \cdot I_{df}} \quad (7)$$

In equation (7), ω_{hm} symbolizes the speed of rotation of the pump/motor element, ω_{aks} the rotation speed of the wheel axle. The connection between the rotation speed of the wheel axle and the vehicle's linear speed is calculated as shown in equation 8 under the assumption that the wheels do not slip.

$$\mathcal{V} = \omega_{aks} \cdot r \quad (8)$$

The MATLAB-Simulink model relating the wheel axis with the hydraulic pump/motor element is shown in Figure 8.

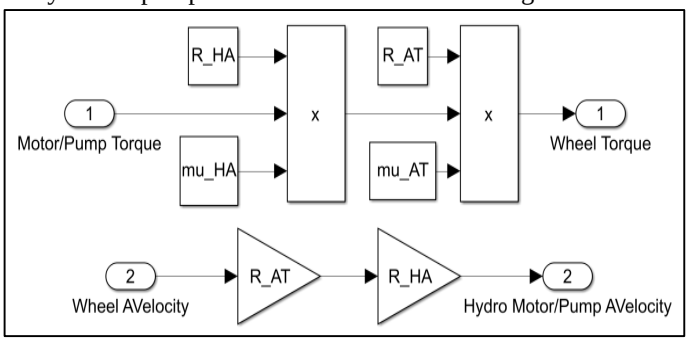

Figure 8. Hydraulic pump/motor element and wheel axle relationship MATLAB-Simulink model.

2.3. Forces applied by the hydraulic system

In hydrostatic regenerative braking systems, the torque necessary for the movement and braking of the vehicle is provided by the hydraulic pump/motor element.

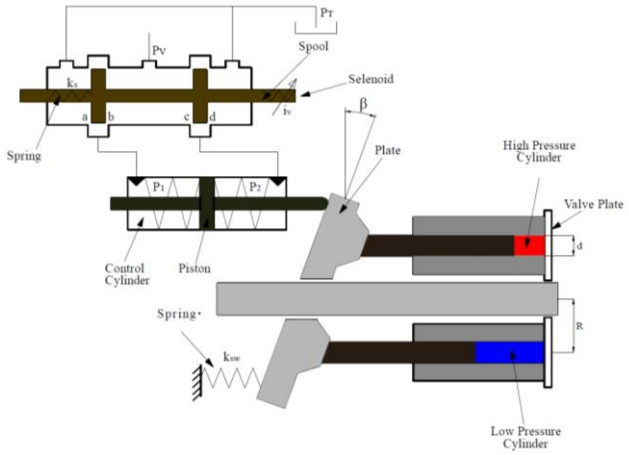

Figure 9. Variable Displacement pump/motor component scheme [11].

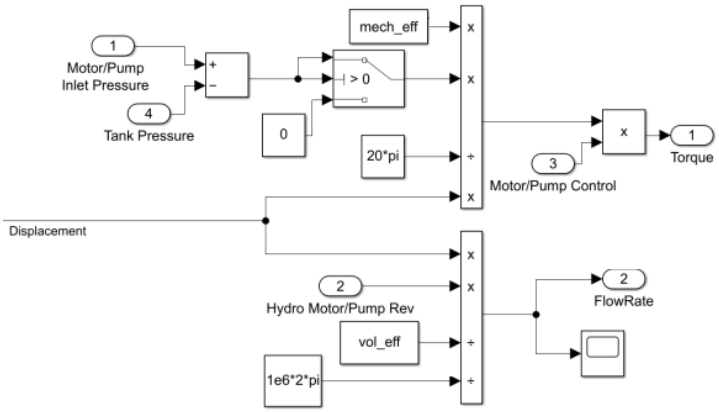

Figure 10. Hydraulic Pump/Motor Element Simulink Model

One of the ports on this element is connected to the battery, the other to the oil storage tank. The pressure difference between the input and output ports enables the hydraulic pump/motor element to generate torque.

The flowrate and output torque of the hydraulic pump/motor component shown in Figure 9 can be adjusted by changing the displacement. The displacement is controlled by changing the angle of the swash plate inside the pump/motor element. A proportional control valve is used to control the angle of the swash plate. While no current is applied to the solenoid on the control valve, the valve that is in balanced position under the spring force keeps the piston that moves the plate in its normal position. The control of piston is achieved by applying current to the solenoid on the valve [11]. The torque reproduced by the hydraulic pump/motor element can be calculated as shown in the equation (9).

$$T_{hm} = \frac{\Delta p \cdot \forall \cdot \eta_{mh}}{20\pi} \quad (9)$$

In the equation 9, the pressure difference between the ports of the Δp pump/motor element, ∀ displacement, η_{mh} mechanical output is expressed. The 20π expression contained in the denominator ensures that the result is obtained in Nm when Δp is expressed in bar units and ∀ is expressed with $(cm^3)/\text{rev}$.

If the pressure at the input port is greater than the output port (transmission of the oil in the accumulator to the storage tank), the hydraulic pump/motor element operates in motor mode. The torque produced in motor mode is of a positive sign and is transferred to the wheel axle by means of powertrains to move the vehicle, as expressed in equation (6). If the pressure at the output port is greater than at the input port (transmission of oil in the tank to the accumulator), the pump/motor component is operating in pump mode. The torque reproduced in pump mode is of a negative sign and is again transmitted to the wheel axle to create a braking effect in the vehicle as expressed in equation (6).

An another important variable related to the hydraulic system is flowrate. Determination of the flowrate is necessary to calculate the power consumed or produced by the hydraulic pump/motor element, to predict losses to the system and to determine the oil transferred to or removed from the accumulator. The flow of the pump/motor component can be calculated as shown in the equation 10.

$$Q = \frac{\forall \cdot \omega_{hm}}{\eta_{vol} \cdot 10^6 \cdot 2\pi} \quad (10)$$

In equation 10, η_{vol} represents volumetric efficiency. The $10^6 \cdot 2\pi$ factor in the denominator ensures that the result is obtained with the m^3/s. unit when calculations are carried out with ω_{hm} expressed in rad/s and the ∀ expressed in $(cm^3)/\text{rev}$. units.

2.4. Modeling of hydraulic accumulator

In the hydraulic energy retrieval system being investigated in this study, energy is stored through a hydraulic accumulator during hydrostatic regenerative braking. In the accumulator consisting of a liquid and a gas chamber, energy is stored by compression of the inert gas [12]

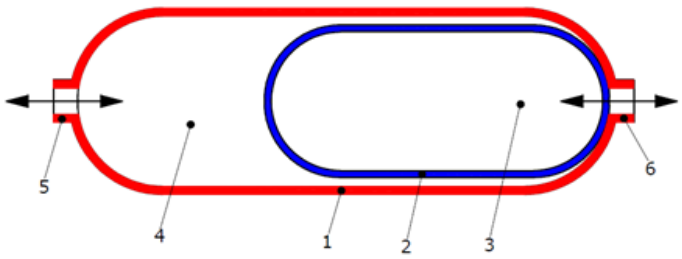

Figure of 11. Balloon hydraulic accumulator

Table 3.Basic parts of hydraulic accumulator.

1	Accumulator Housing
2	Elastic membrane (bladder)
3	Gas Part (inert/nitrogen gas)
4	fluid part (hydraulic fluid/oil)
5	hydraulic fluid/oil input ports
6	Inert/nitrogen gas input ports

Figure 11 shows a simplified representation of the hydraulic accumulator with a bladder. The gas and liquid inside the accumulator are separated by the elastic membrane (Figure 11(2)). Before connecting accumulator to the system (when there is no oil in the liquid chamber, the gas chamber (Figure 11(3)) is filled with an inert gas, usually nitrogen, through the gas input port (Figure 11(6)). While there is no oil in the accumulator yet, the pressure produced by the gas when the elastic membrane covers the entire accumulator volume is called the pre-charge pressure. After the accumulator is connected to the system, if the system pressure passes the pre-charge pressure, the oil passes from the hydraulic fluid input port (Figure 11(5)) to the liquid chamber (Figure 11(4)). The oil flowing inside the accumulator causes gas to be compressed and increases in pressure. When the system pressure decreases again, the oil in the accumulator is transferred back to the system through the compressed gas. The pressurized oil delivered to the system is converted into motion energy through the hydraulic motor.

In this study, it was assumed that the gas in the accumulator is an ideal gas that undergoes in a polytropic process during expansion or compression in energy storage and regeneration phases. This assumption is usually shown to give sufficiently accurate results in applications where nitrogen gas is used and there are no very high pressures [13]. The ratio of pressure and volume of an ideal gas undergoing a polytropic process relationship is expressed as shown in equation 11.

$$p_0 \cdot V_0^{\gamma} = p_1 V_1^{\gamma} = constant \quad (11)$$

In equation 11, p_0 represents the pre-charge pressure of the gas; p_1 represents any pressure. V_0, refers to the volume of the gas at the pre-charge pressure, i.e. the total capacity of the accumulator; V_1, represents the volume that the gas covers at p_1 pressure. γ symbolizes the polytropic gas constant. For the nitrogen gas undergoing adiabatic process, the value γ=1.4 is compatible with experimental studies [13]. The volume of the gas in the accumulator for any pressure can be calculated by rearranging the equation (11).

$$V_1 = \left(\frac{p_0}{p_1}\right)^{1/\gamma} \cdot V_0 \quad (12)$$

After the accumulator is connected to the system, the change of gas volume occurs with oil entering the inside. Since the total volume of the accumulator is fixed, the instantaneous volume of oil contained in it can be calculated by deducting the volume of gas calculated using the equation (12) from the total accumulator volume.

$$V_y = V_0 - V_1 \quad (13)$$

The pressure of the oil must pass the gas pressure in order for getting oil to enter the accumulator. If the pressure of the oil exceeds the gas pressure, the pressures will be equal.

$$p_y = p_g \qquad ; p > p_0 \quad (14)$$

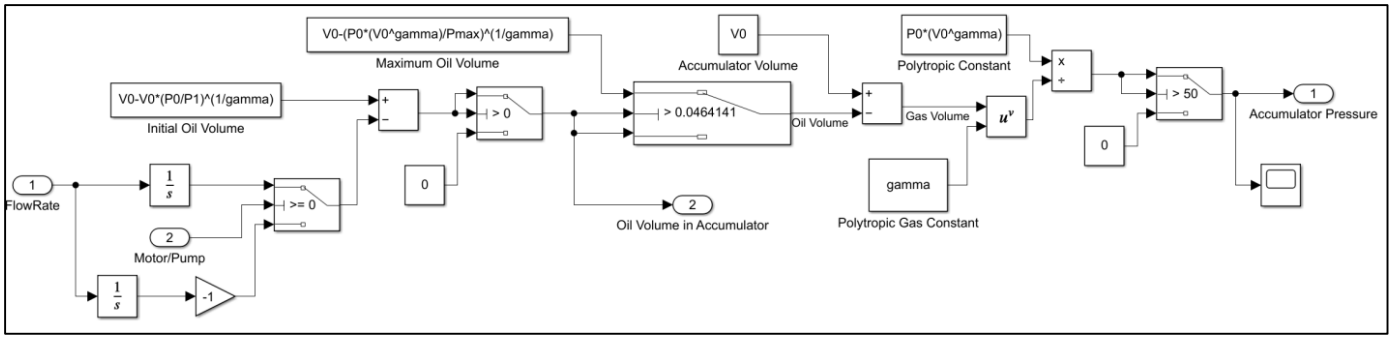

Figure 12. The Matlab-Simulink hydraulic accumulator model

In equation 14, p_y is the oil pressure; p_g is the gas pressure. During the modeling of the volume and pressure of the oil in the accumulator, the speed of the pump/motor element is determined according to the vehicle speed with the help of a model associated with the wheel axle speed and the turn rate of the pumps/motor elements is calculated and the depletion of oil entering or leaving the accumulator is computed. The change in the accumulator oil volume is calculated by taking the integral during the simulation period of this accumulator. Interesting model is shown in Figure 12.

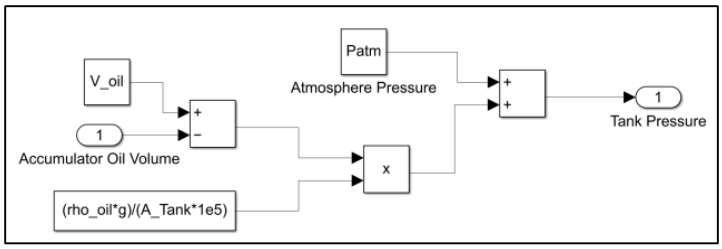

Figure 13. Hydraulic oil tank MATLAB-Simulink model

2.5. Modeling of hydraulic tank

In this study, losses in elements such as the hose and junctions inside the hydraulic system were neglected, and the pressures in the input and output ports of the hydraulic pump/motor element were assumed to be equal to the pressure of the element to which they were connected. Together with this assumption, when the pump/motor element is in motor mode, the pressure of the input port is equal to the oil pressure in the accumulator; the output port pressure is equivalent to that of the oil in the oil storage tank. In the pump mode, the situation will be the opposite. Since the modeled system belongs to vehicles with high mass, the volume of the accumulator that will be used for energy storage will be large, so it is predicted that the volume of the oil tank should be large. Therefore, the volume of oil in the tank's creation pressure is also considered. The pressure of the oil in the tank can be calculated as shown in the equation (15).

$$p_t = \left(V_t - V_y\right) \cdot \frac{\rho_y \cdot g}{A_t \cdot 10^5} + p_{atm} \quad (15)$$

The equation (15), V_t represents the total volume of oil in the system, the ρ_y represents oil density, A_t represents the base area of the oil tank, and the p_{atm} represents the atmospheric pressure.

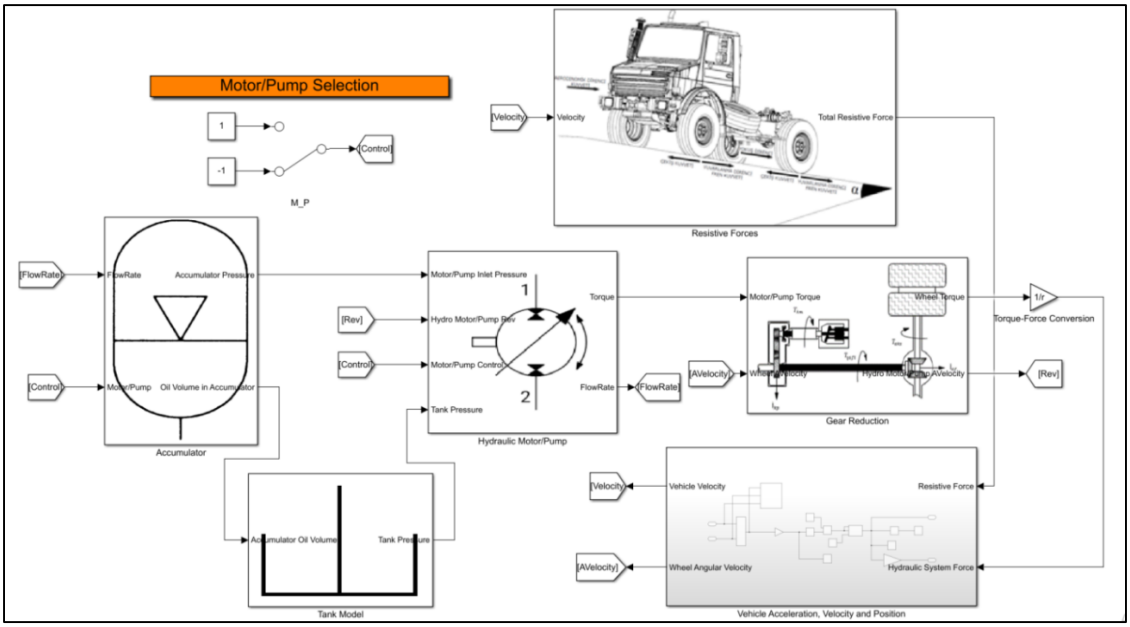

Figure 14. The MATLAB-Simulink model

2.6. Simulink Model

In the Simulink model presented in the Figure 14, the combination of the resistive forces acting on the vehicle with the calculated force is primarily based on the pressure difference between the ports of the hydraulic pump/motor element and thus the acceleration of the vehicle is determined. The velocity is calculated using the acceleration of the car, and the velocity data of the vehicle is also used to calculate the speed of the pump/motor shaft using the pump / motor element-wheel axle relationships. The fixed mathematical relationship it has with the wheel axis because the pump/motor element is directly mechanically connected will be basis for the modeling study. This relationship provides the ability to examine the flowrate and flow direction in the hydraulic system regardless of parameters such as the acceleration or deceleration of the vehicle or the mode in which the engine/pump element is running (braking in pump mode, drive in motor mode) and therefore the charging state of the accumulator.

In order to be able to examine various scenarios during the simulation work, the initial conditions of the vehicle need to be determined in addition to the fixed parameters. Among these conditions, the most important is the charge state of the accumulator and the initial velocity the vehicle has. For example, defining the velocity of the vehicle at the beginning of the simulation as greater than 0 can simulate the braking state and take into consideration the changes as the accumulator reaches its maximum charge. Easily the speed of the vehicle can be simulated by initially defining as 0 and the changes can be studied as how much the vehicle can be accelerated with various accumulator charging volumes.

3. Simulation Study and Results

Two scenarios have been selected to study the performance of the hydraulic system and its impact on the movement of the vehicle.

(1) At the beginning of the simulation, the speed of the vehicle is considered to be 0 (not moving) and the maximum working pressure of the charging pressure element in the accumulator is 400 bar. In this scenario, the displacement of the variable hydraulic pump/motor component is moved linearly from completely off position to completely on position in 2 seconds. Under the mentioned conditions, the pressure pump/motor element in the accumulator without using any control method has been studied for variables such as the movement and flow in the hydraulic system resulting from the forces applied to the vehicle while running in motor mode.

(2) At the beginning of the simulation, the speed of the vehicle is assumed to be 15 m/s (~50 km/h) and the charge pressure in the accumulator is equal to the pre-charge pressure (no oil in the accumulator). In this scenario, the displacement of the variable hydraulic pump/motor component is moved linearly from completely off position to completely on position in 2 seconds. Under the mentioned conditions, variables such as the pressure in the accumulator, the force applied to the vehicle when the pump/motor element is operated in pump mode without the use of any control method, and the flow in the hydraulic system, such as pressure variations have been examined

The results of the simulation of scenario (1) are placed in Figure 15. The graphs in Figures (a), (b) and (c) show the change in the acceleration, speed and position of the vehicle accordingly. Graph (d) shows the time-related change in the pressure of the oil stored in the hydraulic accumulator and the resistive forces acting on the vehicle. The flow rate of the hydraulic pump/motor element is presented in the graph (e).

When the results of the simulation are examined, the oil pressure in the accumulator is reached to the pre-charge pressure in 23 seconds. If the oil pressure reaches or falls below the pre-charge pressure, it means that the accumulator is empty because the oil cannot get into the accumulator. This point is shown in graphs with dashed lines.

At the beginning of the simulation, the accumulator produces the highest torque that can be produced at full charge (highest pressure), which can also be deducted from equation 9. The torque produced at this point is limited to the displacement of the pump/motor element. As in practical applications, it is not possible to instantly bring the highest volume of the displacement in terms of equipment safety, the opening time of 2 seconds is defined in the simulation. The effect of this situation can be seen in the graph (a) as the second of the point where the acceleration is the highest. After this point, as a result of the pressure in the accumulator, the torque reproduced by the pump/motor element continuously decreases. By the 15th second, even though the accumulator pressure is more than 80 bars, the torque is not enough to overcome the resistive forces on the vehicle and the vehicle begins to slow down.

As a result of the simulation, it was observed that the vehicle could reach a speed of approximately 4 m/s by moving from stand still. This speed value usually corresponds to the first gear range of vehicles such as heavy trucks and indicates that the system can be applied to vehicles frequently stopping and taking off such as garbage collection trucks.

In addition, the simulation study concluded that the hydraulic system has a significantly high flowrate and elements with high fluid conductivity should be used.

The results of the simulation of scenario (2) are placed in Figure 16. The graphs in Figures (a), (b) and (c) provide information about the vehicle's acceleration, velocity and position, as in the previous scenario. The graphs (d) and (e) show the resistive forces affecting the vehicle with the characteristics of the hydraulic system, such as accumulator pressure and flow.

As a result of the simulation, the oil pressure in the hydraulic accumulator reached 400 Bar, the maximum working pressure (full charge) in approximately 5 seconds. This point is shown in graphs with vertical dashed lines. After the oil pressure in the accumulator reaches its highest degree, the oil transmitted to the accumulator by the pump/motor element will virtually be evacuated to the tank through a pressure relief valve and if desired can continue to brake due to the load produced by this valve.

As in the previous scenario, the displacement of the pump/motor component was fully opened in 2 seconds. The effect of this situation can be observed in the graph (e) as the rate value calculated using the equation (10) depending on speed and

displacement has the highest value in 2 seconds.

When the simulation results have been examined, it was found that in the case of braking, the flow rates were higher than the starting state, even over 600 L/min. While the effects of this situation are not observed in the model in which hydraulic losses are not taken into account, it would in practice result in very high energy losses and unacceptable warming in hydraulic oil if the loss is considered to be proportional to the square of the flowrate , especially in the case of the use of elements with inadequate flow transmissive rates. Transmissive elements that can meet the flowrate observed, especially in the braking phase, are not serially produced. The resulting model can also be used for the development of the controller that will keep the hydraulic pump/motor element flowrate at an acceptable level.

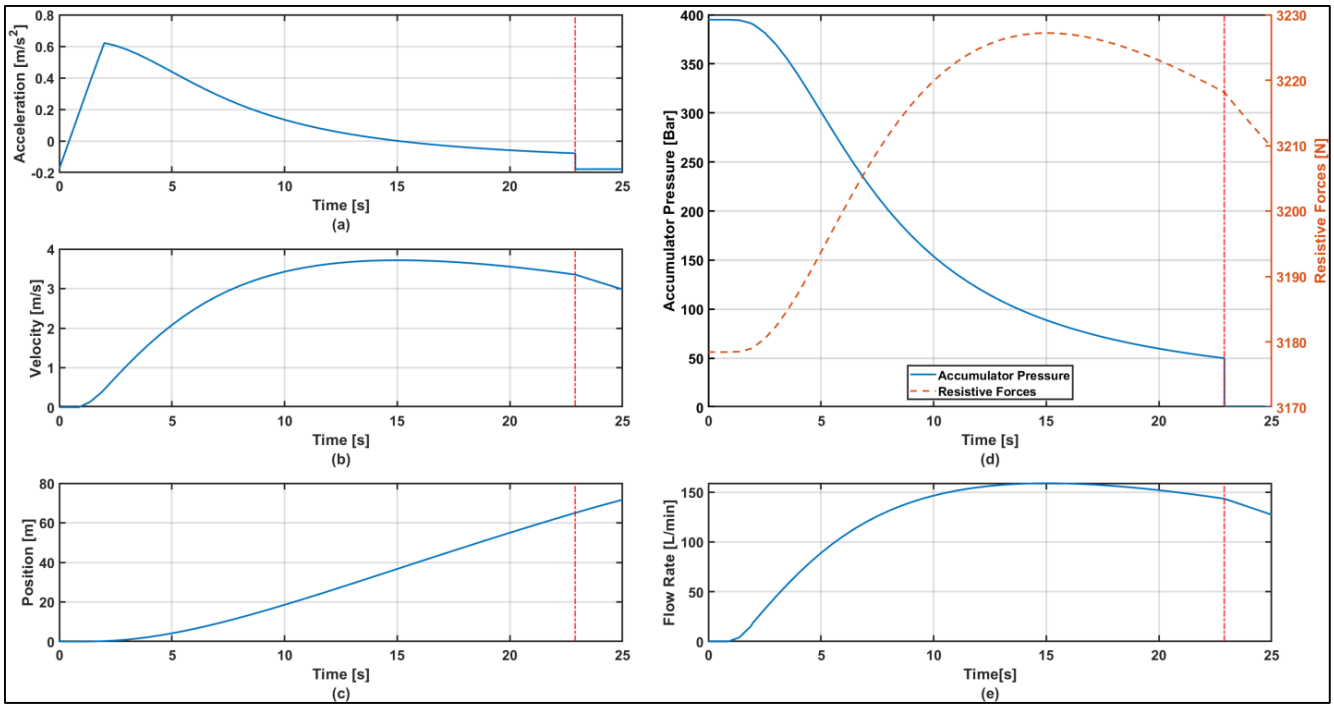

Figure 15. Vehicle Acceleration Graphs.

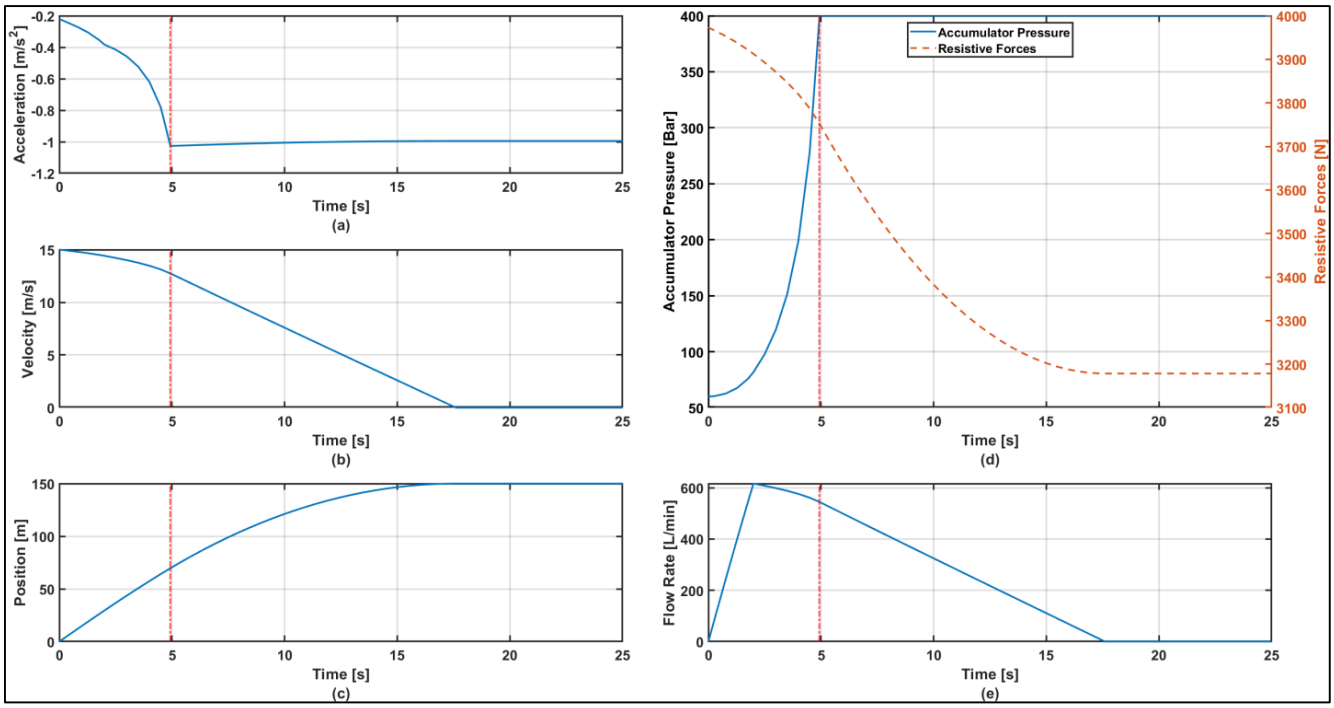

Figure 16. Vehicle Braking Graphs.

Table 4. Simulation of Parameters

Parameters	Value
Cross-sectional area of the vehicle	7.20598 m^2
Oil tank base area	0.25 m^2
Coefficient of air resistance	0.8
Rotation Resistance Coefficient [14]	0.018
Hydraulic pump/motor maximum dispalcement	80 cm^3/rev
Pre-charge pressure	50 bar
Maximum accumulator pressure	400 bar
Atmospheric pressure	1 bar
Vehicle drivetrain- hydraulic pump/motor transmission rate	4.11
pump/motor-vehicle transmission rate	7
Accumulator Volume	0.06 m^3
Total oil volume	0.1 m^3
Gravitational acceleration	9.81 m^2/s
Polytropic gas coeffıcient	1.4
Vehicle weight	18000 kg
Mechanical efficiency of the pump/motor	0.9
Vehicle-wheel drive efficiency	0.8
Pump/Motor-Vehicle shaft gearbox Ratio	0.8
Wheel diameter	0.5715 m
Air density	1.225 kg/m^3
Oil density	700 kg/m^3
Pump/Motor Volumetric Efficiency	0.9

4. Conclusion

In this study, the factors that will have a serious impact on the operation of the system, such as hydraulic losses, the compressibility of oil under high pressure have been ignored, the resistive forces acting on the vehicle have been modeled in a quite simple way. Thus, the resulting model was used to calculate the resistance forces that will result from the effects of different parameters such as weight, load and movement rather than overlap with practical applications, and to determine the hydraulic elements such as the pump/motor element, the accumulator, necessary to overcome these forces. In addition to the determination of the elements to be used, it is possible to determine the valves that will be used with the prediction of variables such as the displacement of the hydraulic system. Within these model outputs, the experimental system that will be created for verification studies can ensure that the losses are modeled according to reality and the validity of assumptions such as the assumption that the gas in the accumulator is ideal can be examined within this study. The model developed in line with the experimental results will form the basis for work to be carried out in advanced times such as the development of the controller.

Acknowledgements

The authors express their deepest gratitude to 'Hidroan Ankara Hidrolik Mak. San. Tic. Ltd. Şti.' for the opportunities provided for this study.

Conflict of Interest Statement

Authors declare that there is no conflict of interest in the study.

CRediT Author Statement

Mustafa Karaman: Conceptualization, Methodology, Software, Writing - original draft, Investigation

Salih Korucu: Conceptualization, Supervision, Writing - original draft.

References

1. Hamada, A.T. ve Orhan M.F., An Overview of Regenerative Braking Systems, Journal of Energy Storage, 2022, 1-33.
2. Ramakrishnan, R., Somashekhar, S. Hiremath, Singaperumal, M., Open Loop Dynamic Performance of Series Hydraulic Hybrid System with Hydrostatic Regenerative Braking, Proceedings of Joint Fluids Engineering Conference, Hamamatsu, Shizuoka, Japan, 2011.
3. Baseley, S., Ehret, C., Greif, E., Kliffken, M.G., Hydraulic Hybrid Systems for Commercial Vehicles, Proceedings of Commercial Vehicle Engineering Congress, Illinois, 2007.
4. Rydberg, K.E., Energy Efficient Hydraulic Hybrid Drives, Proceedings of Scandinavian International Conference on Fluid Power, 2009
5. Ho, T.H. ve Ahn, K.K., Design and Control of a Closed-Loop Hydraulic Energy-Regenerative System, Automation in Construction, 2011, 444-458.
6. Shen, W., Jiang, J., Su, X., Karimi, H.R., Control Strategy Analysis of The Hydraulic Hybrid Excavator, Journal of The Franklin Institute, 352 (2015), 541-561.
7. Liu, H., Jiang, Y., Li, S., Design and Downhill Speed Control of An Electric-Hydrostatic Hydraulic Hybrid Powertrain In Battery-Powered Rail Vehicles, Energy, 187 (2019),
8. Ehsani, M., Gao, Y., Longo, S., Ebrahimi, K., Modern Electric, Hybrid Electric, and Fuel Cell Vehicles, CRC Press, New York, 2018.
9. Vatan, O., Modelling and Simulation of Longitudinal Dynamics of Electric Vehicles, ITU Press, İstanbul, 2011.
10. Çetin, S., Seyir Çevrimlerinin Oluşturulmasında Yokuş Direnci Etkisinin İncelenmesi, İTU Press, İstanbul, 2012.
11. Zhou, S., Walker, P., Tian, Y., Zhang, N., Mode Switching Analysis and Control for A Parallel Hydraulic Hybrid Vehicle, Vehicle System Dynamics, 59:6 (2021), 928-948.
12. Jaipal, P.A., Hydraulic Hybrids, KTH Royal Institute of Technology School of Engineering Sciences, ISSN 1651-7660, Stockholm, 2017.
13. Vacca, A. ve Franzoni, G., Hydraulic Fluid Power: Fundamentals, Applications, and Circuit Design, John Wiley & Sons, New Jersey, 2021.
14. Jazar, R.N., Vehicle Dynamics, Springer Science+Business Media, New York, 2014.
15. Vu, N.H., ve Kim, J.W., A Review of Hydraulic Regenerative Braking Systems for Electric and Hybrid Electric Vehicles, Energies, 2021.
16. Zhou, C., Zhang, Q., Sun, Y., Design of an Energy-Saving Hydraulic Regenerative Braking System for a Heavy Mining Truck, IEEE Access, 2021.